Experimental Test of Charge Independence in $n+p \rightarrow d+\pi^0$†

D. F. BARTLETT, C. E. FRIEDBERG, K. GOULIANOS, AND I. S. HAMMERMAN*
Palmer Physical Laboratory, Princeton, New Jersey 08540

AND

D. P. HUTCHINSON
Princeton-Pennsylvania Accelerator, Princeton, New Jersey 08540

(Received 19 December 1969)

The differential and total cross sections for the reaction $n+p \rightarrow d+\pi^0$ were measured for neutron kinetic energies between threshold (275 MeV) and 700 MeV. Results are presented based on 90 000 events. A comparison is made with existing data for $p+p \rightarrow d+\pi^+$ to test the prediction of charge independence, $d\sigma\ (np \rightarrow d\pi^0) = \frac{1}{2} d\sigma (pp \rightarrow d\pi^+)$, at the same c.m. energy and angle. No evidence for a violation is seen. Limits of a few percent are placed on the real part of certain amplitudes for isospin-nonconserving transitions from a study of the symmetry of the angular distributions about $\theta^* = 90°$.

INTRODUCTION

THE charge independence of the pion-nucleon force has been under study since the early 1950's. Yang, in 1952, pointed out that a comparison of the differential and total cross sections for the reactions

$$n+p \rightarrow d+\pi^0 \tag{1}$$

and

$$p+p \rightarrow d+\pi^+ \tag{2}$$

would provide a severe test of charge independence. Neglecting the $n-p$ and $\pi^0-\pi^+$ mass differences, charge independence predicts that the ratio of the differential cross section for reactions (1) and (2), at the same c.m. energy and angle, is equal to $\frac{1}{2}$:

$$d\sigma(np \rightarrow d\pi^0)/d\sigma(pp \rightarrow d\pi^+) = \tfrac{1}{2}. \tag{3}$$

By virtue of the identity of the particles in the initial state of reaction (2), the π^+ angular distribution must be symmetric about $\theta^* = 90°$. Thus, according to (3), the c.m. angular distribution of the π^0 in reaction (1) must also be fore-aft symmetric and any asymmetry must be attributed to isospin-violating transitions.

In this paper, we present the results of an experimental study of reaction (1) for neutron energies from threshold through the peak in the total cross section at $T_n \approx 600$ MeV and we test the following specific predictions of charge independence: (a) that the angular distributions for reactions (1) and (2) are the same at the same c.m. energies, (b) that the ratio of the total cross section for reaction (1) to that of reaction (2) is constant at all energies, and (c) that the c.m. angular distribution for reaction (1) is fore-aft symmetric.

Reaction (2)[1–9] and its inverse,[10–17] the pionic disintegration of the deuteron, have been studied extensively. The differential cross section is nonisotropic with the value at $\theta^* = 90°$ being typically $\frac{1}{4}$ of the value at $\theta^* = 0°$ and 180°. The total cross section also has a pronounced shape, rising from zero at the threshold, $T_p = 285$ MeV, to a broad resonance peak of about 3 mb near $T_p = 600$ MeV [attributable to an intermediate $\Delta(1236)$ state] and then falling by a factor of 10 by $T_p = 1000$ MeV.

Reaction (1) has also been studied previously at these energies. No departure from charge independence has been seen in these measurements,[18–20] the most accurate of which[20] was performed at 600 MeV and claims 20 and 10% uncertainty in the total and the relative differential cross section, respectively.

The data presented in this paper were accumulated in the course of an experiment designed to study the

† Work supported by the U. S. Atomic Energy Commission, under Contract No. AT(30-1)-2137, and by the Office of Naval Research, under Contract No. N0014-67-A-0151-0001.

* Present address: Nevis Laboratory, Box 137, Irvington-on-Hudson, N. Y.

[1] F. S. Crawford, Jr., and M. L. Stevenson, Phys. Rev. **97**, 1305 (1955).
[2] R. M. Heinz, O. E. Overseth, D. E. Pellett, and M. L. Perl, Phys. Rev. **167**, 1232 (1968).
[3] T. H. Fields, J. G. Fox, J. A. Kane, R. A. Stallwood, and R. B. Sutton, Phys. Rev. **109**, 1704 (1958).
[4] D. V. Bugg, A. J. Oxley, J. A. Zoll, J. G. Rushbrooke, V. E. Barnes, J. B. Kinson, W. P. Dodd, G. A. Doran, and L. Riddiford, Phys. Rev. **133**, B1017 (1964).
[5] K. R. Chapman, T. W. Jones, Q. H. Khan, J. S. C. McKee, H. B. Van der Raay, and Y. Tanimura, Phys. Letters **11**, 253 (1964).
[6] L. G. Pondrom, Phys. Rev. **114**, 1623 (1959).
[7] M. G. Mescheryakov and B. S. Neganov, Dokl. Akad. Nauk SSSR **100**, 677 (1955).
[8] M. G. Mescheryakov, N. P. Bogacev, and B. S. Neganov, Nuovo Cimento Suppl. **3**, 119 (1956).
[9] V. M. Guzhavin, G. K. Kliger, V. Z. Kolganov, A. V. Lebedev, K. S. Marish, Yu. D. Proloshkin, V. T. Smolyankin, A. P. Solokov, and Ts'ui Wa-Ch'uang, Zh. Eksperim. i Teor. Fiz. **46**, 1245 (1964) [Soviet Phys. JETP **19**, 847 (1964)].
[10] R. Durbin, H. Loar, and J. Steinberger, Phys. Rev. **84**, 581 (1951).
[11] D. L. Clark, A. Roberts, and R. Wilson, Phys. Rev. **83**, 649 (1951).
[12] A. M. Sachs, H. Winick, and B. A. Wooten, Phys. Rev. **109**, 1733 (1958).
[13] H. I. Stadler, Phys. Rev. **96**, 496 (1954).
[14] B. S. Neganov and L. B. Parfenov, Zh. Eksperim. i Teor. **34**, 767 (1958) [Soviet Phys. JETP **7**, 528 (1958)].
[15] C. E. Cohen, Phys. Rev. **105**, 1582 (1957).
[16] C. M. Rose, Jr., Phys. Rev. **154**, 1305 (1967).
[17] C. R. Serre, CERN Report No. 68-40, 1968 (unpublished).
[18] R. A. Schluter, Phys. Rev. **96**, 734 (1954).
[19] R. H. Hildebrand, Phys. Rev. **89**, 1090 (1953).
[20] V. B. Fliagin, V. P. Dzhelepov, V. S. Kiselev, and K. O. Oganesian, Zh. Eksperim. i Teor. Fiz. **35**, 854 (1958). [Soviet Phys. JETP **8**, 592 (1959)].

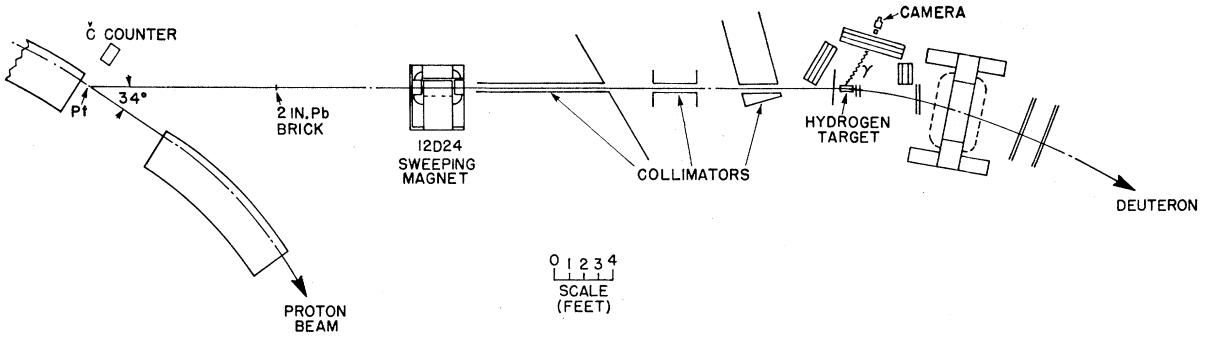

FIG. 1. Experimental arrangement.

radiative neutron capture reaction

$$n+p \rightarrow d+\gamma \qquad (4)$$

for comparison with its inverse reaction as a reciprocity test of time-reversal invariance.[21] For each $d\gamma$ event, we have observed about 70 $d\pi^0$ events in our apparatus. To separate reactions (1) and (4), all events had to be measured and analyzed. As a result, we have obtained about 90 000 examples of $n+p \rightarrow d+\pi^0$, making possible a detailed study of the differential and total cross sections for reaction (1).

EXPERIMENT

The experiment was performed at the Princeton-Pennsylvania Accelerator (PPA).

A beam of approximately 5000 neutrons/sec, produced from an internal Pt target, was defined at an angle of 34° relative to the circulating 3-GeV proton beam. A 2-in.-thick lead brick followed by a sweeping magnet eliminated γ rays and charged particles. The beam illuminated a 3-in.-diam circle on a 4-in.-long liquid-H_2 target placed 51 ft away from the Pt target. Figure 1 shows the experimental arrangement. Since the internal proton beam of the PPA consists of bunches <1 nsec wide and 66 nsec apart, the energy of our neutrons could be determined by measuring the time elapsed between the production of the neutron at the internal target, signaled by a pulse at the Čerenkov counter viewing this target, and the passage of a deuteron through a counter placed immediately after our hydrogen target. The neutron time of flight was determined to ± 0.85 nsec leading to an accuracy of a few percent in the neutron energy ($\Delta T/T = 0.05$ at $T_n = 600$ MeV). The energy spectrum of the neutrons in our beam was measured by a group[22] studying n-p scattering in the same beam but further downstream. This spectrum is shown in Fig. 2.

The apparatus, designed to study reaction (4), was capable of measuring the velocity and momentum vector of the charged particle (deuteron) and the direction of the photon (see Fig. 3). For all neutron energies studied, deuterons from reactions (1) and (4) emerge from the target at lab angles less than 15° and with momenta between 450 and 1500 MeV/c. These were detected in a spark-chamber spectrometer. The momentum of the deuteron was measured by four 0.001-in. aluminum-foil spark chambers placed on either side of a magnet having a bending power of 12° for 1 GeV/c. Most of the deuteron flight path was in helium at atmospheric pressure to reduce multiple scattering. To separate deuterons from protons we recorded the time of flight of the charged particle between counters D_1 and D_{2-4}.

Photons from the decays of the π^0's were converted in three lead-plate spark-chamber arrays. Each of these

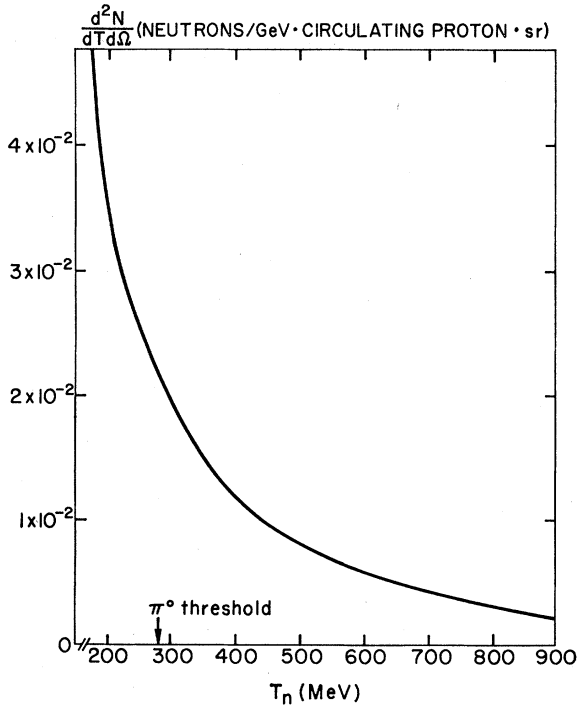

FIG. 2. Neutron spectrum.

[21] D. F. Bartlett, C. E. Friedberg, K. Goulianos, I. S. Hammerman, and D. P. Hutchinson, Phys. Rev. Letters **23**, 893 (1969); **23**, 1205(E) (1969).

[22] R. E. Mischke, P. F. Shepard, and T. J. Devlin, Phys. Rev. Letters **23**, 542 (1969).

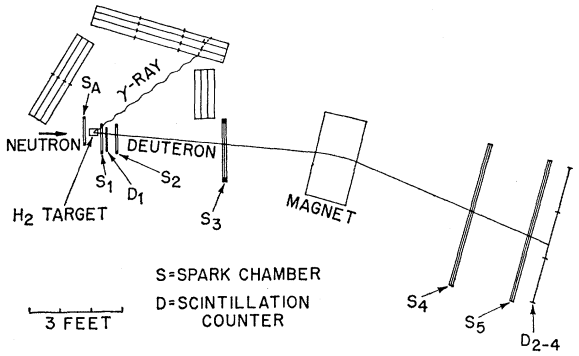

FIG. 3. Apparatus (top view). Counters D_{2-4} are 18 in. high.

arrays consisted of 12 gaps, had an active height of 18 in., and was approximately three radiation lengths thick (see Fig. 4). For triggering each array, scintillation counters were placed before the first gap (anti counters), and after the fourth, eighth, and twelfth gaps (γ counters). The "lead" plates were made of 0.080-in. lead sheet sandwiched with epoxy between two 0.025-in. Al sheets for rigidity. The first plate of each array was $\frac{3}{16}$-in. Al and converted only about 6% of the photons. Thus, the gap following this plate was used as an "antigap" to register charged particles which may have missed being detected by the anti counter. The plate separating the last two gaps before a γ counter was only $\frac{1}{16}$-in. Al and thus all showers that triggered a γ counter had at least two successive sparks. This feature of the construction of the spark chambers facilitated the calculations of the detection efficiency of the photons, in which it was assumed that any shower triggering a γ counter yields a visible "track," defined as two or more successive sparks. Only the conversion point of the γ ray was used in the reconstruction of the events.

To trigger the chambers, we required a coincidence between (a) a signal from D_1, (b) a prompt signal from any of the 18 γ counters, (c) a delayed pulse from D_{2-4}, falling within a broad "deuteron gate," but (d) no signal from any anti counter.

The chambers were photographed by a single 35-mm camera placed effectively 40 ft above the apparatus (actually, the camera was at beam level and the apparatus was reflected in a mirror placed 24 ft above the floor). Side views of all chambers were provided by mirrors attached to the sides of the chambers at 45°. Each picture also recorded the times of flight of the neutron and the deuteron.

Approximately 1.7 million pictures were taken with the hydrogen target full and 50 000 with the target empty. Of these, 1.1 million were in a format suitable for measurement by an automatic flying-spot digitizer.

MEASUREMENT OF EVENTS

The scanning and measurement of the film were performed partly by a computer-controlled flying-spot scanning system (SPASS)[23] and partly by hand. A

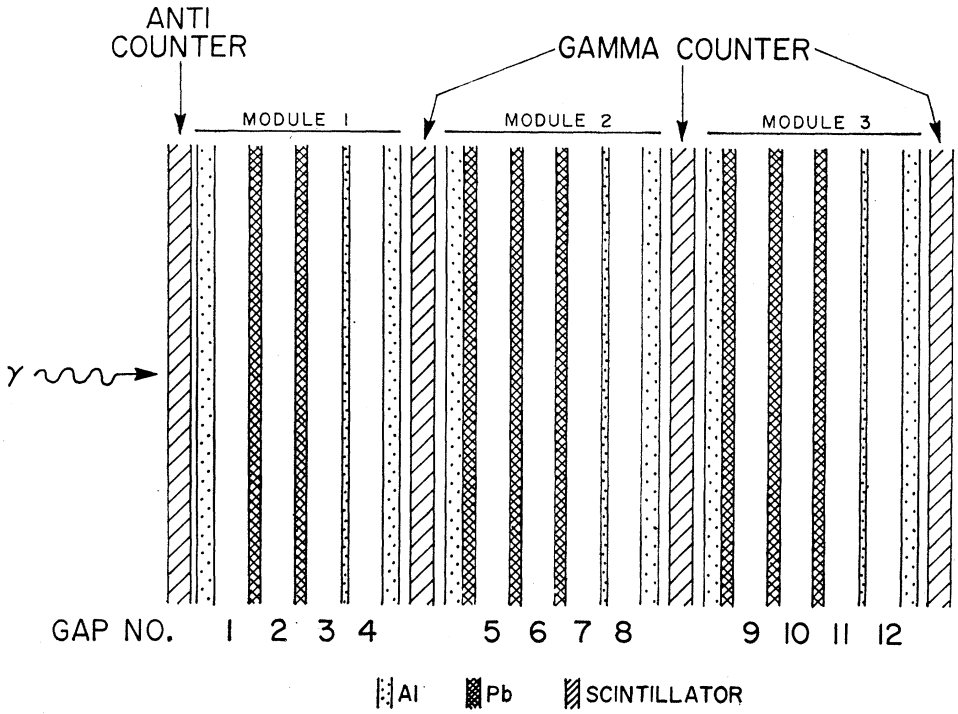

FIG. 4. Spark-chamber array.

[23] For a description of the SPASS system, see C. F. Friedberg, thesis, Princeton University [Elementary Particles Laboratory Technical Report No. 5, PURC-2137-13, 1969 (unpublished)].

total of 1.26 million pictures were scanned, about one-eighth of them manually. A picture was measured if it contained (a) one clearly recognizable charged-particle track in the deuteron chambers and (b) one or two γ showers, each at least two gaps long. SPASS scanned and measured the events at the rate of one per second, approximately 100 times faster than the hand-operated machines. In addition, the SPASS measurements were about twice as accurate as the HAND measurements, but difficulty with faint sparks resulted in a slightly smaller fraction of events being accepted by SPASS than by the scanners. A systematic study showed that, insofar as quantities of importance in this experiment are concerned, the two sets of data are identical.

A total of 530 000 pictures were measured. Culled immediately from this sample were 27 000 events containing two γ rays, 100 000 events having a spark in the thin chamber S_A located upstream of the hydrogen target, and 25 000 events having a track beginning in the first gap of a γ spark-chamber array. The sample was further depleted by discarding 60 000 events in which the charged particle leaving the hydrogen target was a proton rather than a deuteron. This separation, based on a comparison of the measured momentum with that obtained from the time-of-flight system assuming the charged particle to be a deuteron, could be made with better than 99.9% reliability (see Fig. 5).

The remaining events were subjected to fiducial cuts. An event was rejected if the deuteron headed towards the γ-chamber side of the beam or was outside

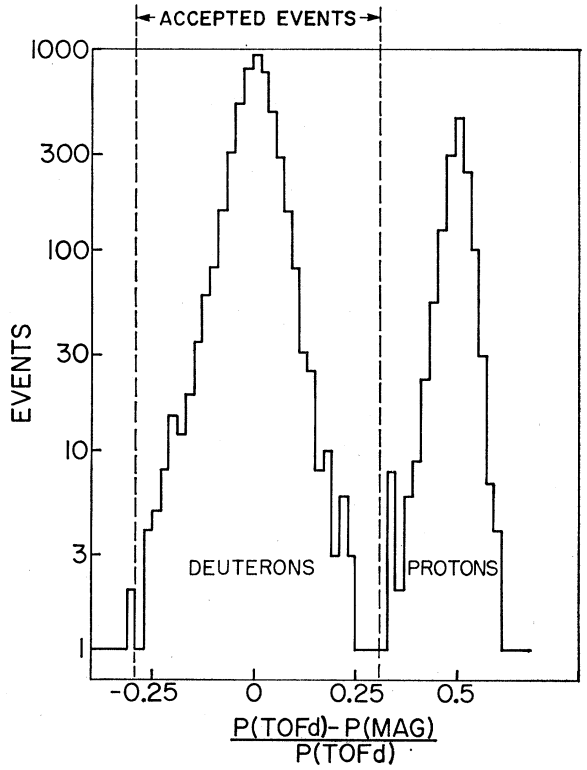

FIG. 5. Deuteron-proton separation (6300 events).

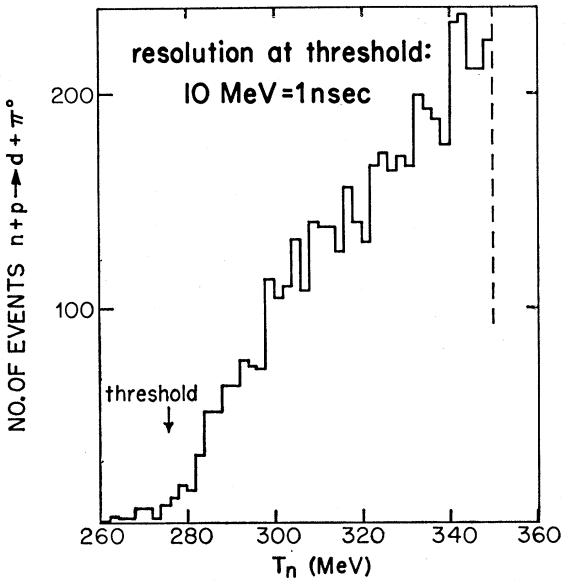

FIG. 6. Calibration of TOFn from π^0 threshold.

a restricted vertical fiducial region defined before the magnet. The reason for accepting deuterons in a central region only was primarily to minimize the difficulty in the calculation of the efficiency of the apparatus arising from the vertical focusing of the particles in the fringe field of the 18-in.-gap magnet. This cut eliminates deuterons going to approximately the top and bottom 3 in. of spark chamber S_5. An inefficiency found at the top and bottom 2 in. of S_5 (possibly caused by vapors released by the sealant) makes the rejection of the events effected by this cut even more desirable. Similarly, fiducial cuts were made in the location of the γ-ray conversion point so that a line from any point in the hydrogen target going to any point in the fiducial volume would pass through all three layers of γ counters. This was done to facilitate calculation of the γ-ray efficiency. About 95 000 events survived these cuts. Of these, 5000 are examples of $n+p \rightarrow d+\gamma$ and their extraction from the dominant $d\pi^0$ "background" has been discussed in a previous paper.[21,24] The remaining 90 000 events are examples of $n+p \rightarrow d+\pi^0$.

DATA ANALYSIS

The analysis involves reconstruction and identification of the events, transformation to the c.m. system, and calculation of the efficiency of the apparatus.

(*a*) *Reconstruction.* The quantities measured were the times of flight of the deuteron (TOFd) and of the neutron (TOFn), the direction of the deuteron and its bending angle in the magnet, and the γ-ray conversion

[24] About 3500 of these events were produced by neutrons of energy less than 400 MeV and were extracted from the sample on an event-by-event basis. The remaining 1500 events were treated statistically and therefore remained as background in the $d\pi^0$ sample. A correction was made for this background before the $d\pi^0$ angular distributions were plotted.

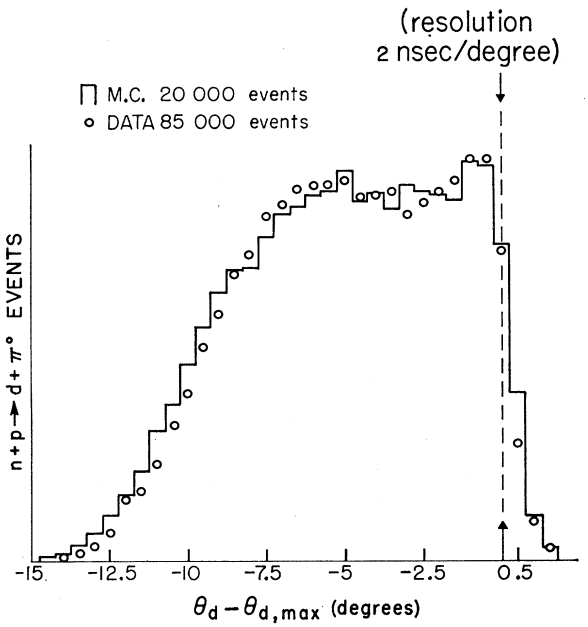

FIG. 7. Calibration of TOFn from maximum lab deuteron angle.

point. TOFd was determined, over the 15-ft flight path between counters D_1 and D_{2-4}, to an accuracy of ± 0.9 nsec, corresponding typically to an accuracy of $\pm 3\%$ in the momentum of the particle, P (TOFd) (assumed to be a deuteron). The deuteron direction was measured to an accuracy of about $\frac{1}{4}$ of a degree. Its momentum as determined by the magnetic spectrometer, P(mag), was measured to about $\pm 3\%$. For a deuteron, P(TOFd) should equal P(mag), but for a proton it should be twice as large. Thus, the protons were removed from the sample by a comparison of the two momenta P(TOFd) and P(mag) (Fig. 5). The direction of the γ ray was obtained to an accuracy of a few degrees by joining the conversion point with the center of the extrapolated trajectory of the deuteron in the H_2 target. While knowledge of the γ direction is not necessary for the reconstruction of the events, a study of the angle between the γ ray and the reconstructed direction of the π^0 helps in the event identification. In addition, the π^0-γ angle determines the energy of the photon and, thus, it can be used to check the efficiency of the γ chambers as a function of γ-ray energy, as it will be described later. Finally, TOFn was measured to ± 0.85 nsec over the neutron's 51-ft flight path. (A correction was made for the fact that the particle traversing the 0.57-ft distance from the H_2 target to D_1 was a deuteron of known velocity.) The above time resolution corresponds to an accuracy of a few percent in the neutron momentum ($\Delta p/p \approx 4\%$ at $T_n = 600$ MeV). The measurement of TOFn was calibrated periodically in the course of the experiment by removing the lead filter from the beam and thus allowing γ rays ($\beta = 1$) to convert in a lead sheet placed in front of our H_2 target. As we see later, this calibration is very important for the correct reconstruction of the events and hence it was checked in two different ways, using a very pure sample of $n+p \to d+\pi^0$ events. One check is provided by seeing that the time of flight of the neutron at the observed π^0 threshold is in fact the appropriate one for a 275-MeV neutron (see Fig. 6). The other checks that the maximum observed deuteron angle in the lab is the correct one for the calculated neutron energy (see Fig. 7). It can be seen from the figures that a systematic error in the TOFn smaller than 0.5 nsec could only be detected with difficulty. This must be kept in mind, since such an error would affect the distributions we are trying to measure in this experiment.

(*b*) *Event identification.* First, using the measured neutron and deuteron momenta for each event, we calculated the mass of the missing particle:

$$M_x^2(n,d) = (E_n + M_p - E_d)^2 - (\mathbf{p}_n - \mathbf{p}_d)^2. \quad (5)$$

The results of this calculation were compared with the expected missing-mass distribution for reaction (1) and found to agree very well. The distribution of the π^0-γ angles also compared well with that predicted by the Monte Carlo program. We concluded that the 90 000 events in question are indeed examples of $n+p \to d+\pi^0$.

(*c*) *Center-of-mass angle.* The c.m. angle of the deuteron θ_d^* can, of course, be obtained directly from laboratory measurements of the neutron momentum p_n, deuteron momentum p_d, and deuteron angle θ_d.

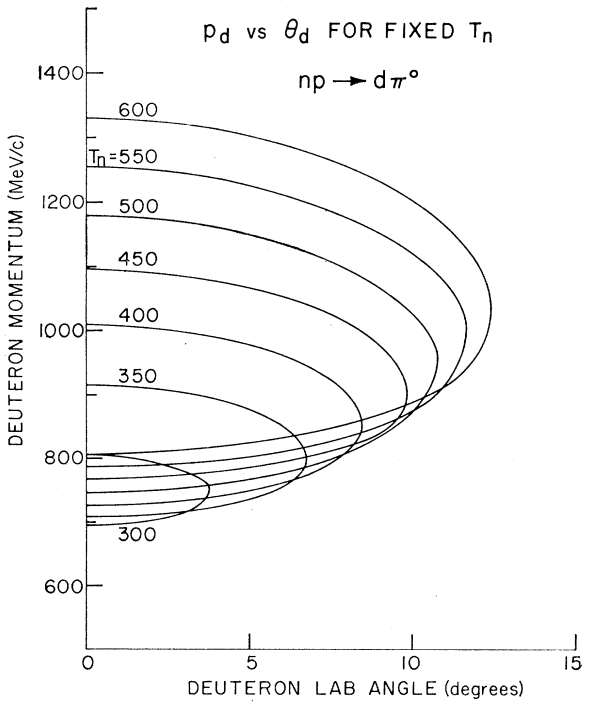

FIG. 8. Kinematics for $n+p \to d+\pi^0$.

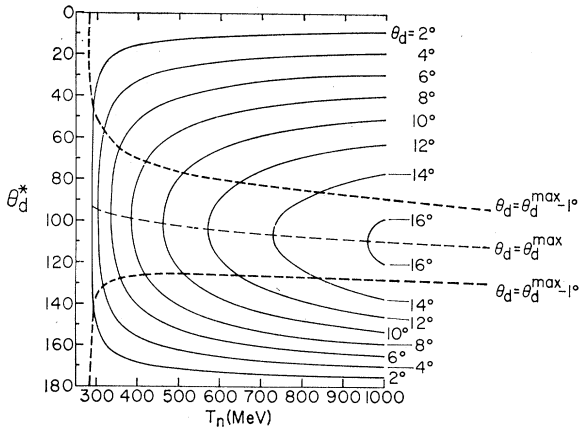

FIG. 9. Center-of-mass angle as a function of θ_d and T_n.

However, the θ_d* calculated in this manner is a sensitive function of p_d and p_n. If one assumes that the neutral particle is a π^0, then by knowing just p_n and θ_d one can predict the two possible values that P_d is allowed to have by the kinematics of $n+p \rightarrow d+\pi^0$ (see Fig. 8). By using the value p_d' that is closest to the measured momentum, one obtains a more accurate value for θ_d* when $\theta_d \lesssim (\theta_d{}^{\max}-1°)$. If θ_d is within 1° from $\theta_d{}^{\max}$, the θ_d* determined using this second method is a very sensitive function of θ_d (see Fig. 9). In this region, it is better to use the measured deuteron momentum to calculate θ_d*. The combination of the two methods leads to c.m. angles with typical statistical accuracy of $\pm 2.5°$.

All events were transformed to the c.m. system using the combined method and were binned according to neutron energy and θ_d*. To determine the differential and total cross sections it is necessary to know the efficiency of each bin.

(*d*) *Efficiency.* A Monte Carlo simulation of reaction (1) was used to calculate the efficiency of the apparatus as a function of c.m. angle and neutron energy. The program predicted the detection efficiency allowing for the number of valid $n+p \rightarrow d+\pi^0$ events lost in the various cuts. Included in this program were the shape of the incident neutron spectrum[22] and the efficiency for the detection of γ rays as a function of their energy and their angle with the spark-chamber plates. A separate Monte Carlo program[25] was used for the calculation of the γ-ray efficiency. The results of this calculation, shown in Fig. 10, were checked by a method using the events themselves. The π^0 direction and momentum was reconstructed and "π^0 beams" were defined by selecting events with the π^0 found to be within a certain narrow angular and momentum range. For each such beam, the π^0-γ angle gives the momentum of the γ-ray. Thus, results of the γ-ray efficiency calculation could be checked by comparing

[25] Based on the technique of J. Butcher and H. Messel [Nucl. Phys. **20**, 15 (1960)].

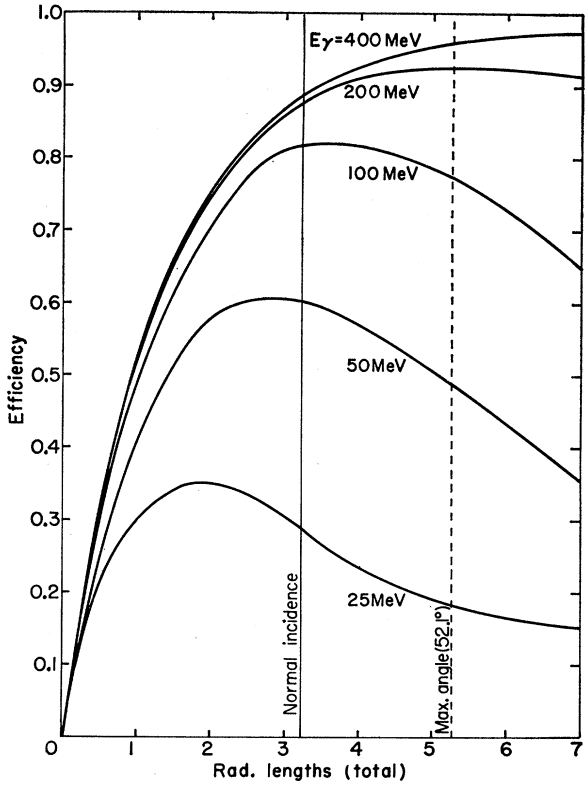

FIG. 10. γ-ray efficiency.

the measured distribution of the π^0-γ angle of the events in a "π^0 beam" with a Monte Carlo generated distribution assuming the calculated efficiency. Figure 11 shows such a comparison.

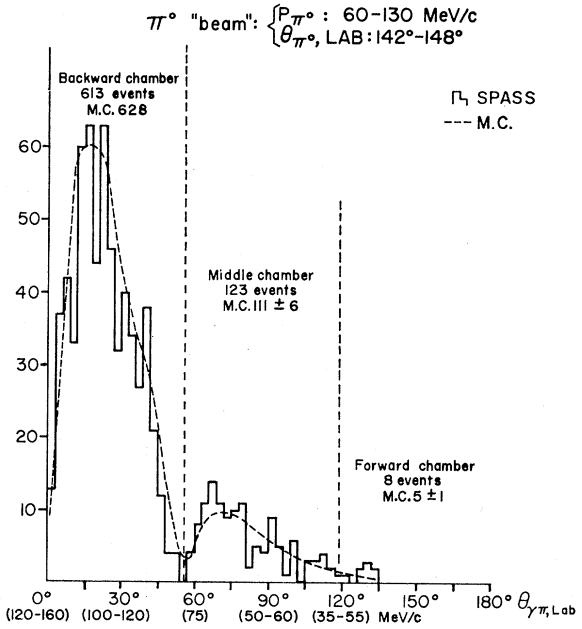

FIG. 11. Example of "π^0 beam" method for checking calculation of γ-ray efficiency. M.C. indicates Monte Carlo calculation.

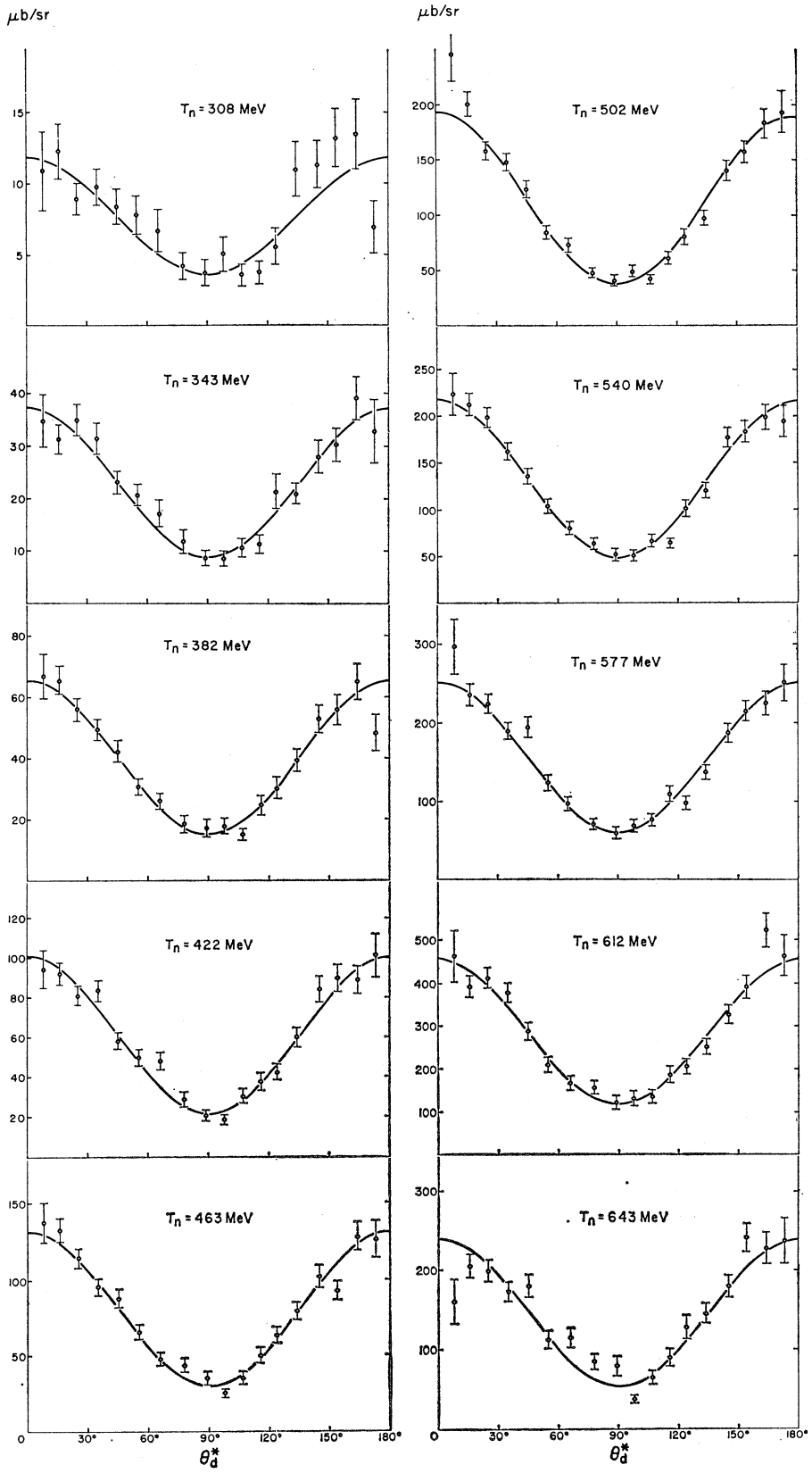

FIG. 12. Center-of-mass differential cross sections for $n+p \rightarrow d+\pi^0$, normalized so that the total cross section be $\frac{1}{2}$ of that for $p+p \rightarrow d+\pi^+$ at $T_n \sim 600$ MeV. The curves are fits to the data in the form $f(\theta) \sim A+\cos^2\theta$.

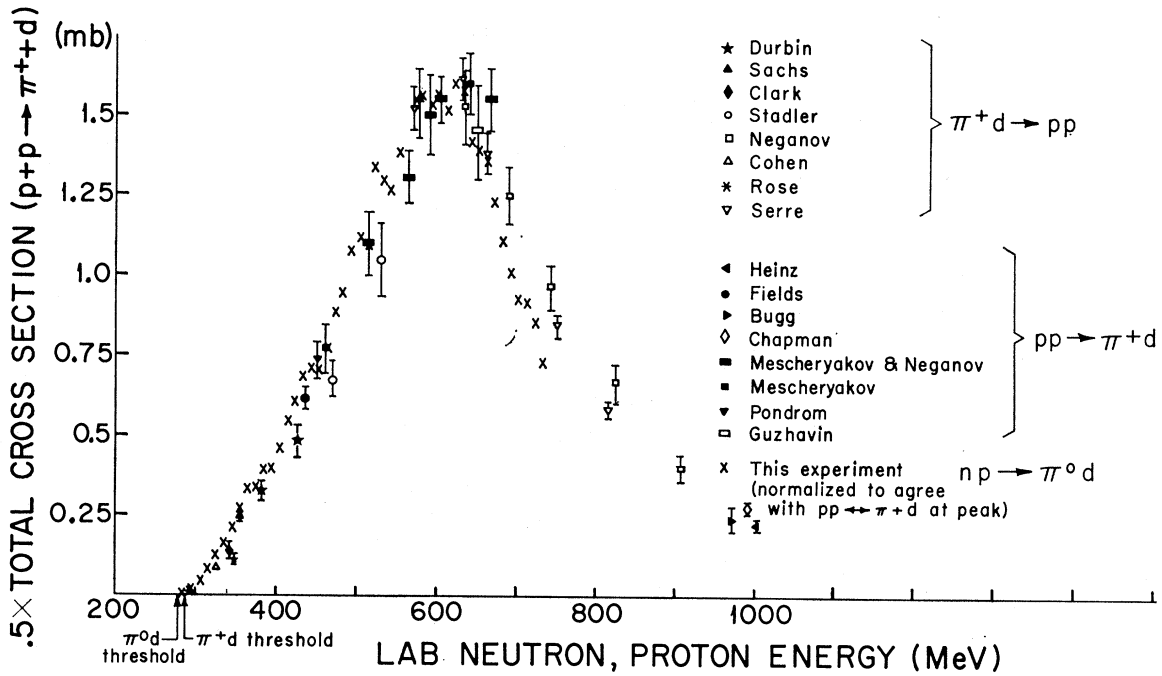

FIG. 13. Total cross section for $n+p \rightarrow d+\pi^0$, normalized to $\frac{1}{2}$ of that for $p+p \rightarrow d+\pi^+$ at the peak.

Typical detection efficiencies for $d\pi^0$ events within the cuts were about 2.5%. By dividing the number of events in a given bin by the efficiency for that bin, we obtained unnormalized angular distributions, one for each energy interval. Since the relative normalization was correct, the variation of the total cross section with energy can be obtained by integration of these distributions.

A final note concerns the "target-empty" events. Analysis of these events showed that 2% of all our events did not originate in the H_2 target. About 70% of these can be attributed to the hydrogen content of the Mylar walls of the target housing and therefore should be "good" events. The remainder 30% (~0.6% of all events) must have originated in the heavier nuclei of the target walls. Since the energy and angular distributions of the target-empty events were not significantly different from those of the regular events, no correction was made for this background.

RESULTS

The deuteron c.m. angular distributions for $n+p \rightarrow d+\pi^0$ are presented in Fig. 12 for 10 energy intervals from threshold ($T_n=275$ MeV) to $T_n=680$ MeV. The energy distribution within each interval is roughly Gaussian with a full width varying from 30 MeV near the threshold to 60 MeV at the highest energy. The mean neutron energy for each interval is shown in each graph. The total cross sections are presented in Fig. 13. Knowledge of the shape of the neutron spectrum resulted in a correct relative normalization for our data as a function of neutron energy. For the purpose of comparison with the charged reaction (2), we have arbitrarily adjusted our over-all normalization so that our total cross section at the resonance peak be one-half that for $p+p \rightarrow d+\pi^+$, as predicted by charge independence.

The errors shown in all our points are statistical. A discussion of systematic errors and their effect on the results will be given in the next section. The statistical errors are too small to be shown in the total-cross-section points, but can readily be inferred from the fluctuations in the points themselves plotted in 10-MeV bins; here, the systematic errors will prove to be more important.

For comparison with previous results, a fit to our data points was determined in the form

$$f(\theta)=a_2(a_0/a_2+\cos^2\theta), \quad A=a_0/a_2. \tag{6}$$

The curves in Fig. 12 are the best fits of Eq. (6) to the data. The coefficients A for the various energy intervals are given in Table I. The errors quoted are statistical. The estimated systematic error in the coefficients is 24% (see discussion in the next section). Included in Table I are the energies of the pion, for comparison with data from $\pi^++d \rightarrow p+p$, and the goodness of the fit in units of χ^2 per degree of freedom, based on the statistical errors in the data points. The χ^2 is consistently high for all energies and does not improve with the addition of a $\cos^4\theta$ term in the form

$$f(\theta)=a_2[a_0/a_2+\cos^2\theta+(a_4/a_2)\cos^4\theta], \quad A=a_0/a_2, \quad B=a_4/a_2. \tag{7}$$

A large χ^2 could arise from systematic effects. The

TABLE I. Coefficient of angular distributions. $f(\theta)\sim A+\cos^2\theta$.

T_n (MeV)	T_π (MeV)	A[a]	χ^2 per degree of freedom
308	11	0.440±0.094	1.58
343	28	0.306±0.043	0.97
382	48	0.297±0.034	1.07
422	68	0.278±0.027	1.45
463	88	0.292±0.027	1.59
502	108	0.242±0.021	1.79
540	127	0.288±0.025	1.25
577	145	0.316±0.028	1.52
612	163	0.348±0.035	1.19
643	178	0.290±0.031	3.08

[a] Errors are statistical only. The systematic error in A is estimated to be 24% (see discussion in text). The average value of A over $350<T_n<650$ MeV is $\bar{A}_n=0.280\pm0.065$ (error includes systematic uncertainty).

size of these effects does not permit us to make a meaningful statement about the presence of the coefficient B [Eq. (7)] in our differential cross sections.

Charge independence requires that the angular distribution be symmetric about 90°. To obtain a measure of the symmetry of our experimental distributions about 90°, we made a fourth-order Legendre polynomial fit to the data, including odd terms in $\cos\theta$, in the form

$$f(\theta)=k(P_0+\alpha_1P_1+\alpha_2P_2+\alpha_3P_3+\alpha_4P_4). \quad (8)$$

We then calculated the forward-backward asymmetry parameter defined as

$$A_{\rm fb}=(F-B)/(F+B), \quad (9)$$

where F and B represent the integral of Eq. (8) from 0° to 90° and from 90° to 180°, respectively. The parameter $A_{\rm fb}$ is given in Table II. The average asymmetry is about (1±1.9)%. The values of $A_{\rm fb}$ and of their errors presented in Table II have been corrected for the following two systematic effects: (a) Deuteron stripping in the matter before the magnet results in loss of the event. The probability of stripping is momentum-dependent, ranging from 3% for $p_d=700$ MeV/c to 1% for $p_d=1400$ MeV/c. Thus, for all neutron energies, deuterons with c.m. angle near 180° are lost by this process more often than deuterons with c.m. angle near 0°. The effect on the coefficient A of the $\cos^2\theta$ terms is negligible (~0.5%), but this process, if not corrected for, would have contributed about +1% to the asymmetry parameter $A_{\rm fb}$. (b) Another systematic effect for which $A_{\rm fb}$ has been corrected has to do with an error in neutron-energy assignment caused by pulses from fast deuterons in D_1 being detected about 0.15 nsec later than pulses from slow deuterons (owing to the difference in ionization loss). Because of the steep slopes of the total cross section on either side of the resonance peak, this timing error contributes about +1% (−1%) to $A_{\rm fb}$ for events to the left (right) of the resonance peak, while the contribution at the peak is negligible. This error does not affect significantly the coefficients of the angular distributions or the shape of the total cross section.

TABLE II. Fore-aft asymmetry $A_{\rm fb}$.

T_n (MeV)	$A_{\rm fb}$ (%)[a]	T_n (MeV)	$A_{\rm fb}$ (%)
308	1.8±4.2	502	2.4±1.6
343	2.0±2.7	540	1.8±1.6
382	1.3±2.2	577	2.6±1.6
422	−1.3±2.0	612	−0.2±1.8
463	1.5±1.8	643	−1.5±2.1

[a] The errors are statistical only, after correction for deuteron stripping and time slewing. Average asymmetry over all energies: $\bar{A}_{\rm fb}=0.01\pm0.019$; with all systematic errors included: $\bar{A}_{\rm fb}=0.01\pm0.028$.

DISCUSSION OF RESULTS

We attempt, first, to place limits on the effect of all possible sources of systematic error known to us. The following such sources have been considered:

(*i*) *Polarization of the neutron beam.* In a separate *n-p* elastic scattering experiment, we have measured the polarization of the incident neutrons in our beam transverse to their production plane and found it to be +0.045±0.02 (the positive sign means that more neutrons have spin up than down). This value can cause a maximum deviation from the unpolarized cross section of about 2% at 90° [26] resulting in a 2% error in the coefficient A.

(*ii*) *Neutron energy.* An upper limit of 0.4 nsec is assigned to the error in the neutron time of flight. This corresponds to a 4-MeV uncertainty in the location of the threshold (Fig. 6) and 0.2 degrees in the determination of the maximum deuteron lab angle (Fig. 7). An arbitrary decrease of the neutron time of flight by 0.4 nsec increases the neutron energy by about 12 MeV at $T_n=600$ MeV and thus affects the shape of the total cross section. In addition, such a shift decreases the coefficient A by about 20% and gives rise to an asymmetry of −1%.

(*iii*) *γ-ray efficiency.* We estimate that the error in the calculation of the ratio of the detection efficiency for γ's from backward to forward pions could be as large as 3%. This error leads to a 1.5% asymmetry ($A_{\rm fb}$). The effect on A is negligible.

(*iv*) *Deuteron angle.* The lab angle of the deuteron could conceivably have been systematically mismeasured by as much as 1 mrad. This is about ¼ of the random error and causes at most a 7% error in A.

(*v*) *Deuteron momentum.* An error in the deuteron momentum affects only lab angles with $(\theta_d^{\max}-\theta_d)<1°$. A generous 1% systematic increase of p_d has a 10% effect on A, and produces an asymmetry of +1%.

(*vi*) *Deuteron gate.* In order to eliminate protons of high velocity, a gate was used in the deuteron trigger. Unfortunately, this gate also eliminated some of our deuterons affecting the results in the higher-energy intervals. About 20% of the high-energy (forward) deuterons were cut off in the interval labeled $T_n=643$

[26] This estimate uses the results of an asymmetry measurement by Crawford and Stevenson (Ref. 1) for a polarized beam of $T_p=314$ MeV.

MeV, fewer were cut at the lower-energy intervals. The gate was simulated in the Monte Carlo program and thus its affect was incorporated in the over-all efficiency of the apparatus. However, we estimate that at the highest-energy bin the number of deuterons near $\theta_d=0°$ could still be wrong by about 5%. This leads to 2.5% error in A and causes an asymmetry of 1.3%. For the $T_n=520$-MeV bin, the estimated error in A is about 1% with a 0.6% asymmetry.

In summary, if all the possible systematic errors discussed here are added in quadrature they can affect the coefficient A by 24% of its magnitude and cause a 2.1% asymmetry. The largest error in A is caused by the uncertainty in the measurement of the neutron time of flight. Such an uncertainty would, in addition, distort the shape of our total cross section, a fact which must be kept in mind while comparing our distributions with those from reaction (2).

The three experiments[18–20] which have studied the reaction $n+p\rightarrow d+\pi^0$ previously report the following values for the coefficient A:

Other $np\rightarrow d\pi^0$ experiments.

Experiment	T_n(lab) (MeV)	A
Schluter (Ref. 18)	392	$0.28_{-0.14}{}^{+0.26}$
Hildebrand (Ref. 19)	400	0.21 ± 0.06
Fliagin *et al.* (Ref. 20)	600	0.220 ± 0.022

Our value for A (see Table I) is roughly constant with energy. If the systematic error is incorporated into the random error and the results averaged over the energies from 350 to 650 MeV, we obtain $\bar{A}_n=0.280\pm0.065$. This value is a little higher than, but does not disagree with, the value by Fliagin *et al.*, claiming the best accuracy. It should be noted that in the experiment by Fliagin *et al.* only counters were employed and, in particular, that the angular resolution of the deuteron counters was 25 mrad in the laboratory. Thus, the mean deuteron angle within the 25-mrad bin was not known *a priori*, and, therefore, a large systematic error may have to be incorporated into the value of ±0.022 quoted above.

The shape of our total cross section is compared with the cross section for $p+p\rightarrow d+\pi^+$ (and $\pi^++d\rightarrow p+p$, using time-reversal invariance) in Fig. 13. For the purpose of comparing shapes, we have adjusted the normalization to make the cross section agree at the peak of the resonance. One can detect that our points are systematically shifted to the left, towards lower neutron energies. A small part of this shift may be attributed to the difference in the phase space available to reactions (1) and (2) owing to the $\pi^0-\pi^+$ mass difference, while the major part of the shift may well be due to a misalignment of the calibration of the neutron timing. Decreasing the neutron time of flight by 0.35 nsec, a value within the systematic error discussed in (ii), shifts our points towards higher neutron energies and brings the shape of our cross section into very good agreement with that of reaction (2).

The coefficients A of our angular distributions from the fits to $f(\theta)\sim A+\cos^2\theta$ are compared with those for reaction (2) in Fig. 14. The agreement is good within the errors which include the systematic effects. In the energy range $350<T_n<650$ MeV, the average value of A from reaction (2) is $\bar{A}_p=0.240\pm0.015$, while our average value is 0.280 ± 0.065. It is interesting that the

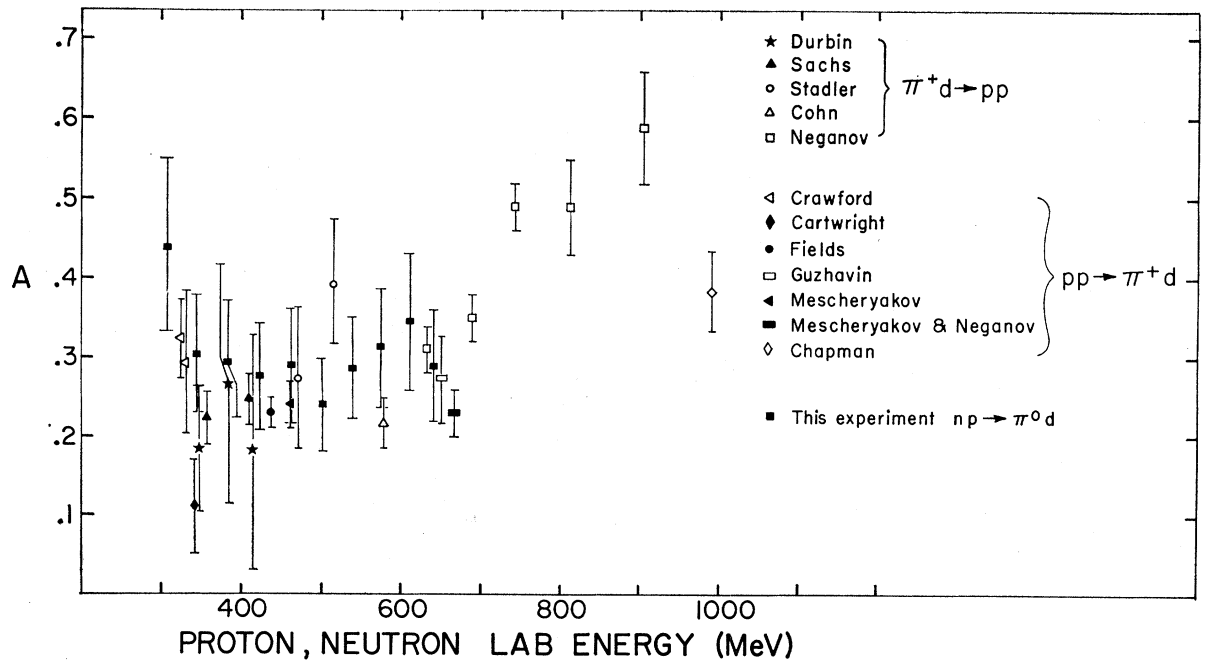

FIG. 14. The coefficient A from the fit to $f(\theta)\sim A+\cos^2\theta$, as a function of energy. Errors include all systematic effects.

0.35-nsec shift necessary to bring the shapes of the total cross sections in agreement also changes our value of $\bar{A}_n$ to 0.232, resulting in better agreement with reaction (2). Another way of expressing this observation is that if one were to assume that charge independence holds for the total cross sections and adjusted the TOFn to make the shapes agree, one would get a value $\bar{A}_n=0.232\pm0.029$ (no error due to TOFn misalignment but all other systematic errors included), in excellent agreement with the value of 0.240 ± 0.015 for reaction (2).

The average forward-backward asymmetry over our energy region has the value $\bar{A}_{\rm fb}=0.01\pm0.028$, where the error includes all the systematic effects discussed. This value is not statistically significant and thus only upper limits can be placed on the presence of isospin-nonconserving amplitudes. Some examples are discussed in the Appendix. The 0.35-nsec shift discussed above introduces as asymmetry of -1% and thus reduces our value to $\bar{A}_{\rm fb}=0.00\pm0.028$.

Finally, the absolute value of our total cross section merits some discussion. Although the absolute neutron flux was known,[22] the fraction of events rejected in the scanning stage was too large to be calculated reliably. In addition, one could not know whether some of the events which were rejected after they had been measured were of the $np\rightarrow d\pi^0$ type, or belonged to background; e.g., events with a spark in the chamber S_A before the hydrogen target could either have been "good" events or could have been caused by incoming charged particles. However, the reaction $np\rightarrow d\pi^0$ was studied simultaneously with the reaction $np\rightarrow d\gamma$. Assuming, for the purpose of discussion, time-reversal invariance for the total cross sections in the reactions $n+p\leftrightarrows d+\gamma$ and normalizing our results for $np\rightarrow d\gamma$ to those from $\gamma d\rightarrow np$, we obtain

$$\sigma_t(d\pi^0)=1.5\pm0.3\text{ mb}\quad\text{at}\quad T_n=600\text{ MeV},\quad(10)$$

where the (estimated) error is mostly due to the $\gamma d\rightarrow np$ experiments (see Ref. 24). This is in excellent agreement with the value of 1.5 ± 0.3 mb at the same neutron energy reported by Fliagin *et al.*[20]

CONCLUSION

We find no evidence for violation of charge independence, CI, in comparing reactions (1) and (2) in the energy region from threshold through the peak in the total cross section, $280\lesssim T_n\lesssim700$ MeV. Specifically, the following quantitative conclusions may be drawn from the discussion in the preceeding section:

(*a*) *Absolute cross sections.* From Eq. (10) and from the results appearing in Fig. 13, we find that

$$\sigma_t(d\pi^0)/\sigma_t(d\pi^+)=0.5\pm0.11$$

for neutron energies from 350 to 700 MeV, in agreement with the prediction of CI, Eq. (3). This result is contingent upon the validity of time-reversal invariance in the total cross section for $n+p\leftrightarrows d+\gamma$. Because of the difference in phase space, the prediction of CI may be affected appreciably in the vicinity of the threshold and thus we do not make a comparison of total cross sections for energies below 350 MeV.

(*b*) *Shape of the total cross section.* In Fig. 13, we compare the shapes of the total cross sections as a function of neutron energy for reactions (1) and (2). Again in the range $350<T_n<700$ MeV we observe good agreement to within the $\sim10\%$ errors of the charged reaction.

(*c*) *Angular distributions.* We find no conclusive evidence for a $\cos^4\theta$ term. The coefficients A from the fit to $f(\theta)\sim A+\cos^2\theta$ are compared in Fig. 14. The agreement is good, but the errors in our coefficients are large due to systematics. The variation of A with energy is small. In the region $350<T_n<650$ MeV, our average value is $\bar{A}_n=0.280\pm0.065$ as compared to $\bar{A}_p=0.240\pm0.015$ for the charged reaction.

(*d*) *Forward-backward asymmetry.* The prediction of CI is that the fore-aft asymmetry in the c.m. angular distribution of deuterons be zero. The average asymmetry over our energy range is $\bar{A}_{\rm fb}=0.01\pm0.028$, including systematic effects in the error. This is consistent with zero and, thus, we can only place upper limits to the presence of isospin-nonconserving transitions. In the Appendix, we discuss the isospin-violating transitions $^1P_1\rightarrow{}^3S_1$, $^1P_1\rightarrow{}^3D_1$, and $^1F_3\rightarrow{}^3D_3$. On the basis of the error in our asymmetry, we conclude that the real part of the amplitude for these transitions is, respectively, less than 2.6%, 14.4%, and 1.5%, with 90% confidence, of the amplitude of the dominant $^1D_2\rightarrow{}^3P_2$ transition. This, perhaps, is the most stringent quantitative conclusion about charge independence that can be made on the basis of our data.

Finally, in the spirit of seeking confirmation rather than violation of CI, it is of interest that the systematic shift of the shape of our total cross section towards lower energies may be eliminated by reducing the neutron time of flight by 0.35 nsec, a value within the systematic error. Such a timing shift also brings the coefficient of our angular distributions to $\bar{A}_n=0.232\pm0.029$, in excellent agreement with $\bar{A}_p$, and reduces the value of the fore-aft asymmetry $A_{\rm fb}$.

ACKNOWLEDGMENTS

We wish to thank Michael Gruters for his untiring efforts in the development and operation of our automatic film scanner and David C. Cheng for joining us in measuring the polarization of the neutron beam. We have benefited greatly from the zeal of Professor Milton White and the staff of the Princeton-Pennsylvania Accelerator as well as from the advice of Professor S. Barshay and S. Treiman. Finally, we are indebted to our scanners and the Elementary Particles Laboratory Staff for their continual assistance.

APPENDIX: ISOSPIN-CONSERVING AND -NONCONSERVING TRANSITIONS

Since the total isospin in the final state of reactions (1) and (2) is 1, the initial state must also have isospin 1 if charge independence is valid. For the two nucleons, the $I=1$ state has symmetric isospin wave functions and hence the product of the space and spin wave functions must be antisymmetric. In addition, because of the negative parity of the pion, the orbital-angular-momentum quantum numbers must be odd on one side of the reaction and even on the other and, thus, the total angular momentum can have the values

$$J=L(np)=L(d\pi)\pm 1 \quad \text{(singlet } np \text{ state)},$$
$$J=L(np)\pm 1=L(d\pi) \quad \text{(triplet } np \text{ state)},$$

where $L(np)$ is the initial orbital angular momentum and $L(d\pi)$ is the final orbital angular momentum. Accordingly, we list in Table III the possible transitions for which the angular-momentum quantum number of the pion relative to the deuteron is less than 3. Transitions (i) and (ii) produce uniform c.m. angular distributions. Transition (iii) leads to a distribution $\frac{1}{3}+\cos^2\theta^*$ and thus is the dominant one. The other transitions bring $\cos^4\theta^*$ and higher-order terms into the angular distributions.

A violation of CI would appear as a transition from an $I=0$ initial state to the final $I=1$ state. Table IV summarizes the CI-violating transitions. A violation might be seen as an asymmetry about 90° in the c.m. angular distribution. Such an asymmetry is caused by odd powers of $\cos\theta^*$ which can only result from the interference of CI-conserving and CI-violating transitions. We consider only transitions that interfere with the dominant process ${}^1D_2\rightarrow{}^3P_2$, i.e., transitions (a)–(c). The amplitude for the transition ${}^1D_2\rightarrow{}^3P_2$ is

$$(\sqrt{\tfrac{1}{6}})Y_1^{-1}S_1^{1}+(\sqrt{\tfrac{2}{3}})Y_1^{0}S_1^{0}+(\sqrt{\tfrac{1}{6}})Y_1^{1}S_1^{-1}, \quad \text{(A1)}$$

where Y_l^m are spherical harmonies and S_1^m are the deuteron spin-wave functions. The amplitudes for transitions (a)–(c) are

$$\alpha Y_0^0 S_1^0, \quad \text{(A2a)}$$
$$\beta[(\sqrt{\tfrac{3}{10}})Y_2^{-1}S_1^{1}-(\sqrt{\tfrac{2}{5}})Y_2^{0}S_1^{0}+(\sqrt{\tfrac{3}{10}})Y_2^{1}S_1^{-1}], \quad \text{(A2b)}$$
$$\gamma[(\sqrt{\tfrac{1}{5}})Y_2^{-1}S_1^{1}+(\sqrt{\tfrac{3}{5}})Y_2^{0}S_1^{0}+(\sqrt{\tfrac{1}{5}})Y_2^{1}S_1^{-1}], \quad \text{(A2c)}$$

where the α, β, and γ are complex numbers giving the strengths of these isospin-nonconserving transitions relative to (A1).

We now assume that only two amplitudes are present, (A1) and one of the (A2). For each combination, we obtain the angular distribution

$$f_a(\theta)=\tfrac{1}{3}(1+2|\alpha|^2)+\cos^2\theta+\tfrac{4}{3}\sqrt{2}\cos\theta\ \mathrm{Re}\alpha, \quad \text{(A3a)}$$
$$f_b(\theta)=\tfrac{1}{3}+\cos^2\theta+(2\ \mathrm{Re}\beta/1+|\beta|^2)\times[(5/3)\cos\theta-3\cos^3\theta], \quad \text{(A3b)}$$
$$f_c(\theta)=\tfrac{1}{3}+\cos^2\theta+(8/3)(\sqrt{\tfrac{3}{2}})\cos^3\theta\ \mathrm{Re}\gamma+\tfrac{1}{2}|\gamma|^2(7\cos^2\theta-4\cos^4\theta-1). \quad \text{(A3c)}$$

Assuming that $|\alpha|^2$, $|\beta|^2$, and $|\gamma|^2$ are much smaller than unity, the forward-backward asymmetry, defined as

$$A_{\mathrm{fb}}=(F-B)/(F+B),$$
$$F=\int_0^{\pi/2} f(\theta)d\Omega, \quad B=\int_{\pi/2}^{\pi} f(\theta)d\Omega$$

takes the simple forms

$$A_{\mathrm{fb}}(a)=\sqrt{2}\ \mathrm{Re}\alpha=1.41\ \mathrm{Re}\alpha, \quad \text{(A4a)}$$
$$A_{\mathrm{fb}}(b)=\tfrac{1}{4}\ \mathrm{Re}\beta=0.25\ \mathrm{Re}\beta, \quad \text{(A4b)}$$
$$A_{\mathrm{fb}}(c)=2(\sqrt{\tfrac{3}{2}})\ \mathrm{Re}\gamma=2.45\ \mathrm{Re}\gamma. \quad \text{(A4c)}$$

Thus, a measurement of the fore-aft asymmetry places upper limits to the real parts of CI-violating amplitudes.

TABLE III. $np\rightarrow d\pi^0$ isospin-conserving transitions with $L(d\pi)\leq 3$.

(i) ${}^3P_1\rightarrow{}^3S_1$	(iv) ${}^3P_1\rightarrow{}^3D_1$	(vii) ${}^3F_3\rightarrow{}^3D_3$
(ii) ${}^1S_0\rightarrow{}^3P_0$	(v) ${}^3P_2\rightarrow{}^3D_2$	(viii) ${}^1D_2\rightarrow{}^3F_2$
(iii) ${}^1D_2\rightarrow{}^3P_2$	(vi) ${}^3F_2\rightarrow{}^3D_2$	(ix) ${}^1G_4\rightarrow{}^3F_4$

TABLE IV. $np\rightarrow d\pi^0$ isospin-violating transitions: $(I=0)\rightarrow(I=1)$, with $L(d\pi)\leq 3$.

(a) ${}^1P_1\rightarrow{}^3S_1$	(f) ${}^3D_2\rightarrow{}^3P_2$
(b) ${}^1P_1\rightarrow{}^3D_1$	(g) ${}^3D_2\rightarrow{}^3F_2$
(c) ${}^1F_3\rightarrow{}^3D_3$	(h) ${}^3D_3\rightarrow{}^3F_3$
(d) ${}^3S_1\rightarrow{}^3P_1$	(i) ${}^3G_3\rightarrow{}^3F_3$
(e) ${}^3D_1\rightarrow{}^3P_1$	(j) ${}^3G_4\rightarrow{}^3F_4$